ISSN 1070-3632, Russian Journal of General Chemistry, 2008, Vol. 78, No. 3, pp. 355–367. © Pleiades Publishing, Ltd., 2008.
Original Russian Text © S.V. Shevkunov, 2008, published in Zhurnal Obshchei Khimii, 2008, Vol. 78, No. 3, pp. 372–384.

Stability of Molecular Form of HCl in Water Vapor: A Computer Simulation

S. V. Shevkunov

St. Petersburg State Polytechnic University,
ul. Politekhnicheskaya 29, St. Petersburg, 195251 Russia
e–mail: root@svsh.tu.neva.ru

Received July 13, 2007

Abstract—The free energy and entropy of the dissociation of HCl molecule into ions in water vapor, $HCl(H_2O)_n + mH_2O \rightarrow H_3O + (H_2O)_{n+m}–1Cl^-$, were calculated. The dependences of various parameters on the interionic distance at 273 K and various vapor pressures were obtained. A detailed model taking into account unpaired covalent–type interactions, polarization interactions, charge transfer effect, and hydrogen bonds was applied. The numerical values of the parameters were reconstructed from the experimental data on the free energy and enthalpy of the first reactions of addition of vapor molecules to ions, and also from the results of quantum–chemical calculations of the energy and geometry of locally stable configurations of clusters $HCl(H_2O)_n$. Despite lower internal energy of the dissociated state, the molecular form is absolutely stable in clusters of water molecules. The dissociated state is relatively stable. Accumulation of unrecombined ion pairs in clusters is possible with a decrease in the temperature to 200 K.

DOI: 10.1134/S1070363208030043

The solubility of strong acids and salts in clusters of water molecules attracts attention primarily in the context of atmosphere pollution. Atmospheric moisture exerts a cardinal effect on the state of impurities. Water molecules, having relatively large dipole moments, are drawn into the electric field of dipolar impurity molecules. Hydrogen bonds promote the clusterization. Computer simulation of both atomic [1–7] and molecular [8–18] ions in water vapor shows that, under natural atmospheric conditions, there are no ions free of hydration shells. Actually cluster ions, rather than ions themselves, are charge carriers in the atmosphere.

The presence in the atmosphere of a large set of clusters of water molecules is confirmed by environ–mental studies. In the IR range, the atmosphere has an abnormally strong absorption band corresponding to vibration frequencies of hydrogen bonds [19–23]. Estimating the concentration of clusters of water molecules from the measured absorption intensity leads to values that exceed by 7–8 orders of magnitude the concentration of hydrated ions measured in electrometric experiments. It was concluded from the results of laboratory studies that the major fraction of water clusters in the atmosphere is stabilized in the field of ion pairs.

Apparently, the overwhelming majority of ion pairs in the atmosphere are formed by dissociation of water molecules themselves and poses no environmental hazard. At the same time, the existence of such complexes indicates that aggressive substances like strong acids and salts dissociated into ions and stabilized in clusters of water molecules can also axquire long-lived state. The dissociation of a molecule in a water cluster stimulates its chemical activity as in bulk solutions. The absorption and coalescence of clusters containing dissociated molecules of strong acids favors their concentration in macroscopic drops and fallout in the form of acid rains. In this paper the mechanism of dissolution of strong acids in water clusters is considered, with HCl as an example.

Specific features of dissociation in molecular clusters. The dissociation into ions in solution is due to the fact that the dissociated state is thermodynamically favorable. The entropy of the dissociated state is always higher than that of the bound state, because the dissociation of a compound is accompanied by an increase in the volume of the accessible configuration space. The limiting concentration of a solution is determined by the minimal volume per solute molecule at which an increase in the entropy term *TS* of the free

energy of the system compensates a possible increase in the internal energy U, in order for the Gibbs energy $G = U - TS + pV$ to decrease upon dissociation. In strong solvents, the internal energy decreases upon dissociation, and the substances can be mixed in any proportion. In weak solvents, a decrease in the free energy of the solution is exclusively due to an increase in the entropy, which, in turn, depends on the change in the configuration volume upon dissociation of the compound, i.e., on the solute concentration. In this case, there is an upper concentration limit depending on temperature T, and the solubility of condensed substances increases with temperature, as the contribution of the entropy term to the free energy increases. Inverse temperature dependence of the solubility is observed in dissolution of gases, because in this case the volume of the configuration space, on the contrary, decreases in going to a condensed solution, and the term TS has an opposite sign.

In contrast to bulk solutions, in molecular clusters the entropy term TS of the free energy plays a smaller role because of the microscopic size of the system. The volume accessible to motion within the cluster is limited by the cluster size. Therefore, the dissociation, being thermodynamically favorable in bulk solutions, may be unfavorable in a cluster. This simplified pattern allows understanding of only the principal differences between the dissociation mechanisms in bulk solutions and in clusters. Actually a molecular cluster is always in a thermodynamic equilibrium with the vapor, and dissociation of a molecule dissolved in the cluster is accompanied by variations of the size of the cluster itself owing to capture of molecules from the vapor and their loss. The dissociation of a molecule into ions and fluctuating increase in the interionic distance result in that additional water molecules are drawn into the interionic space and the cluster size increases. In the process, the internal energy of the system decreases. Thus, owing to the correlation between the cluster size and interionic space, the dissociation in clusters may be thermodynamically favorable because of a sharp decrease in the internal energy. On the other hand, the cluster size grows owing to vapor condensation, which inevitably decreases the entropy of the system as a whole. The final result (whether the dissociation is thermodynamically favorable or unfavorable) depends on the balance of the entropy and energy terms. The reaction direction and equilibrium constant depend on the particle type and require detailed study on the microscopic level. At the same time, thermal fluctuations play the decisive role in the dissolution, making it necessary to use a statistical approach. Stochastic methods of computer simulation meet these requirements in the best way.

Locally stable molecular configurations. Interactions in the cluster $H_3O+(H_2O)_nCl^-$ are described using the model developed and described in detail in [24]. The model takes into account Coulomb, exchange, dispersion, and polarization interactions, hydrogen bonds, strong unpaired interactions of the covalent type, and effects associated with charge transfer. The parameter values were set so as to reproduce the experimental enthalpies and free energies of the first addition reactions $Cl^-(H_2O)_{n-1} + H_2O \rightarrow Cl^-(H_2O)_n$ and $H_3O+(H_2O)_{n-1} + H_2O \rightarrow H_3O+(H_2O)_n$ at room tem-perature [25–27], and also the energies of the stable configurations of clusters $H_3O+(H_2O)_nCl^-$, calculated quantum–chemically taking into account zero–point vibration energies [28]. The experimental free energies and enthalpies of hydration of each of the ions, Cl^- and H_3O+, for the first addition reactions are reproduced with an accuracy corresponding to that of the experimental data (fractions of k_BT [24]). Matching with the results of quantum–chemical calculations for stable configurations of $H_3O+(H_2O)_nCl^-$ allowed determination of the numerical values of the parameters of direct interactions between ions and unpaired interactions involving both ions.

The thermal de Broglie wavelength of the water molecule at $T = 273$ K is $\Lambda = h/\sqrt{2\pi m_0 k_B T} \approx 0.3$ Å (where m_0 is the mass of the molecule), and the quantum–mechanical indeterminancy in the spacial orientation $\Lambda_{rot} = h/\sqrt{2\pi I k_B T} \approx 1$ (where I is the moment of inertia of the molecule), which corresponds to approximately 60°. Corrections for the quantum character of molecular motion are implicitly included in the interaction model we use, owing to the procedure of its construction. As quantum corrections are tem-perature-dependent, the interaction model constructed by this procedure is actually a pseudo-potential model. The shortcomings of the model are, on the one hand, the presence of implicit corrections for the quantum character of motion in the interactions of water with ions and, on the other hand, the fact that in direct ion–ion interactions these corrections are taken into account incompletely, because the available quantum–

chemical data allowed only the correction for zero-point vibrations but not for anharmonicity. It is impossible to fully include these corrections, as the required experimental data on the free energies of recombina-tion of ions are lacking because of technical complexity of such measurements. The explicit description of the quantum character of molecular motion can be principally provided by the method of Feynman path integrals [29–35], but the calculation of the intermediate-strength potential in systems with high energy barriers is difficult even within the framework of classical statistics. Going to quantum statistics increases the computation time by at least 1–2 orders of magnitude, so that the calculations become unfeasible.

For $n = 0$ and 1, virtually exact coincidence in energy with the results of quantum–chemical calculations has been attained, and for $n = 2$ and 3, the deviation does not exceed the error of the quantum–chemical calculations themselves, which can be estimated from the scatter of the results obtained in [28] using various modifications of the method. The configurations corresponding to the energy minimum of the clusters $H_3O+(H_2O)_nCl^-$ in the pseudopotential interaction model were obtained by the Monte Carlo method with successive cooling of the system to 0.1 K. All the configurations found in [28] by quantum–chemical calculations for $n = 1$–4 were reproduced by this method, in particular, all the three stable configurations of the cluster $H_3O+(H_2O)2Cl^-$. Although the energies of the first two configurations are 0.7% lower than in [28] and the energy of the third configuration is 0.2% higher, these deviations are of the same order of magnitude as the difference between the results obtained for these structures in [28] by different quantum–chemical methods, D95(p,d) and D95++(p,d), i.e., are similar in magnitude to the errors of quantum–chemical calculations themselves.

Addition of one more water molecules to the cluster $H_3O+(H_2O)2Cl^-$ leads to an increase in the interionic distance from 3.165 to 3.183 Å, with simultaneous shortening of the H_3O+–H_2O distances from 3.114 to 3.029 Å and of the Cl^-–H_2O distances from 3.611 to 3.520 Å. According to [28], in one of the locally stable configurations of $H_3O+(H_2O)_3Cl^-$ the proton of the HCl molecule appeared to be closer to the oxygen atom of the adjacent water molecule (1.092 Å) than to the chloride ion (1.756 Å). Such configurations with the proton transfer are considered in [28] as an evidence for the dissociation of HCl into ions. We can hardly agree with this viewpoint, because true dissociation involves overcoming of long-range Coulomb attraction forces and separation of the ions by the distance at which the energy of their interaction becomes lower than k_BT. The proton transfer to the nearest water molecule should be considered only as the first step of HCl ionization. Analysis of the data of [28] shows that the proton transfer is observed in those configurations in which the chloride ion is coordinated by no less than three protons of adjacent particles. Apparently, protons of adjacent molecules withdraw a part of the excess negative charge of the chloride ion and thus weaken the intramolecular bond in HCl.

If the proton transfer to the nearest water molecule with the formation of hydroxonium ion is the initial step of the HCl dissociation into ions, the next step is insertion of water molecules between the H_3O+ and Cl^- ions, breaking the direct contact of these ions. We term such structures configurations with separated charges.

Similar pattern is observed with the cluster $H_3O+\cdot(H_2O)_4Cl^-$. All the three stable configurations of $H_3O+\cdot(H_2O)_4Cl^-$ obtained by quantum–chemical calculations in [28] are structures with the transferred proton, and two of them are configurations with separated charges. In the pseudopotential interaction model, examples of all the three forms of the cluster can be found: with transferred proton, without transferred proton, and with separated charges (Fig. 1). All the stable configurations are combinations of rings of water molecules linked by hydrogen bonds. With an increase in the cluster size, a tendency to charge separation becomes evident. The most stable structure **A** consists of two rings, H_2O–H_3O+–H_2O– and –Cl^-–H_2O–H_2O–H_2O–H_3O+, with the common unit –H_3O+–H_2O–. Transfer of one molecule from the second ring to the first ring leads to less stable configuration **B**. Configuration **C** contains a closed ring of three molecules without ions, and configuration **D**, two such rings with a common unit. In all the four configurations **A–D**, the chloride ion is coordinated by two protons, and hence these configurations cannot be considered as configurations with transferred proton. The proton transfer in configuration **E** is accompanied by a significant decrease in the energy (by 0.25×10^{-19} J). Similar configuration was obtained in quantum–chemical calculations.

Configurations **F** and **G** in Fig. 1 are examples of structures with separated charges, with the ions

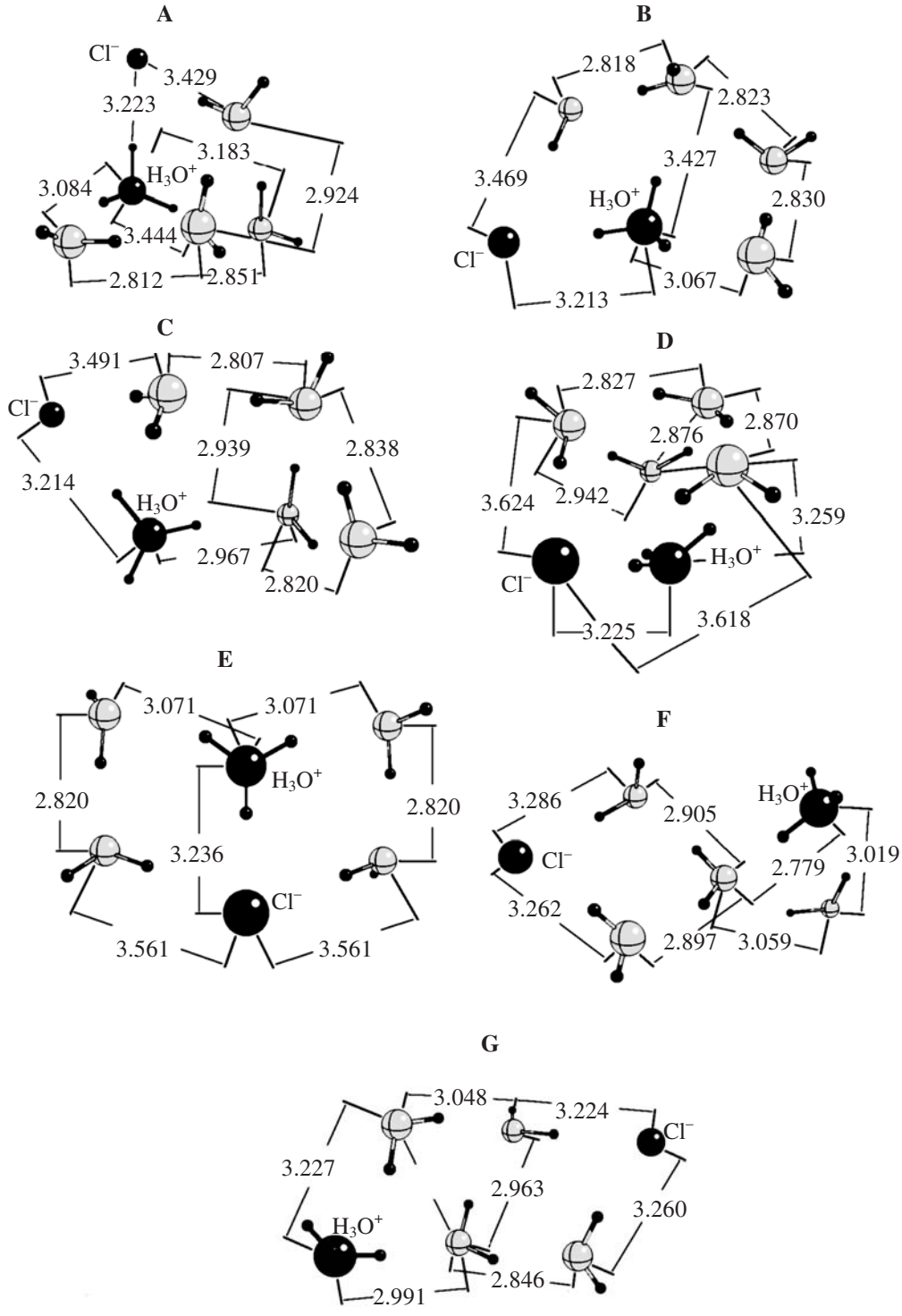

Fig. 1. Stable configurations of the cluster $H_3O+(H_2O)_4Cl^-$ corresponding to local energy minima obtained by quantum–chemical calculations [28] and using the pseudopotential interaction model developed in [24] for simulation at nonzero temperatures. The interatomic distances corresponding to the pseudopotential model are given in Å.

separated by several water molecules. There are no stable configurations in which the ions would be separated by a single water molecule. The energy of the configurations with separated charges is higher by approximately 5×10^{-19} J ~ 130 k_BT, which makes the statistical weights of such states negligible and the charge separation in small clusters impossible. In contrast to quantum–chemical calculations, in the pseudopotential interaction model there are no stable structures in which the two counterions H_3O+ and Cl^- would be separated by a single layer of water molecules linked to protons of the hydroxonium ion. This structure loses stability when taking into account the quantum–mechanical indeterminancy in the molecular orientation and the effect of fluctuating charge, which are implicitly contained in the pseudopotential model.

It can be expected that the main features of the behavior of the energy of locally stable configurations of the cluster $H_3O+(H_2O)_nCl^-$ will also be manifested against the background of thermal fluctuations at finite temperatures. The data obtained suggest that, in separation of the ions, the cluster energy will vary nonmonotonically, passing through a maximum at distances corresponding to one layer of water molecules separating the ions. This distance is approximately 6–7 Å. The results of simulation at finite temperatures confirm this assumption.

Conditions of numerical simulation. The intermediate-strength potential for two ions at a distance R is given by Eq. (1):

$$\Phi(R) = -k_BT\ln [g(R)] + \text{const}, \quad (1)$$

where $g(R)$ is the radial distribution function of ions, depending on temperature T, and k_B is the Boltzmann constant. The spatial derivative of the function $\Phi(R)$ is equal to the mean force acting between the ions, including the interactions via particles of the medium. $\Phi(R)$, accurate to a constant, is the free energy of the system, parametrically dependent on the interionic distance R. In terms of the intermediate-strength potential, the problem of ionic motion in a medium can be reformulated to a simpler problem of the motion of two particles in a vacuum. In particular, the probability of detecting ions in the interval dR at a distance R is given by the formula

$$w(R)dR\infty\exp[-\Phi(R)/k_BT]4\pi R^2dR. \quad (2)$$

The probabilities of dissociation and recombination against the background of thermal fluctuations are expressed by integrals of expression (2) over the corresponding finite intervals of the interionic distance R. According to formula (1), the intermediate-strength potential can be calculated by the Monte Carlo method from $g(R)$, but the direct calculation is impossible if in the dependence $\Phi(R)$ there are relatively high (>10–$100k_BT$) barriers whose overcoming in the course of Markovian wandering becomes improbable, and accumulation of the required volume of statistics for calculating g(R) appears to be impossible. Just such an obstacle arises in attempts to calculate $\Phi(R)$ for ions in molecular clusters. The problem is solved using a special method developed in [36]. The idea of the method consists in introduction of an additional interaction between the ions so as to compensate the existing high barrier in the dependence $\Phi(R)$ and make all the microstates accessible. The compensating potential is calculated by a method that is a combination of the Monte Carlo method with the method of successive iterations. The intermediate–strength potential in the modified system is then recalculated to $\Phi(R)$ for the initial system. The details of the calculation algorithm are given in [36, 37].

For numerical calculation of $\Phi(R)$ in the clusters $H_3O+(H_2O)_nCl^-$ the chloride ion was fixed in the center of a spherical cavity and the hydroxonium ion freely moved inside the cavity in accordance with the equilibrium distribution function at 273 K. The distance R between the ions was counted from the center of the oxygen atom of the H_3O+ ion to the center of the Cl^- ion. Simulation of the material contact with the vapor was performed by the method of the grandcanonical ensemble [38]: The number of water molecules was not fixed but fluctuated in accordance with the Gibbs distribution function and the preset chemical potential of molecules μ. To this end, Markovian steps were made with attempts to throw a water molecule into the cavity or to remove it from the cavity. The details of the algorithm are given in [2]. For the convenience of comparison with the data of a real experiment, the chemical potential was recalculated to the water vapor pressure using the formula for ideal gas (3):

$$p = [8\pi^2k_BT/\sigma\nu_{ref}]\exp(\mu^{conf}/k_BT\}. \quad (3)$$

The configuration part of the chemical potential μ^{conf}, which is the input parameter of calculations [2], is related to μ by Eq. (4):

$$\mu^{conf}(p,T) = \mu(p,T) - [\overline{-k_BT\ln(Z_{tr}^{kin}Z_{rot}^{kin}n_{ref})}], \quad (4)$$

$$Z_{tr}^{kin} = (h/\sqrt{2\pi m_0k_BT})^{-3}, \quad (5)$$

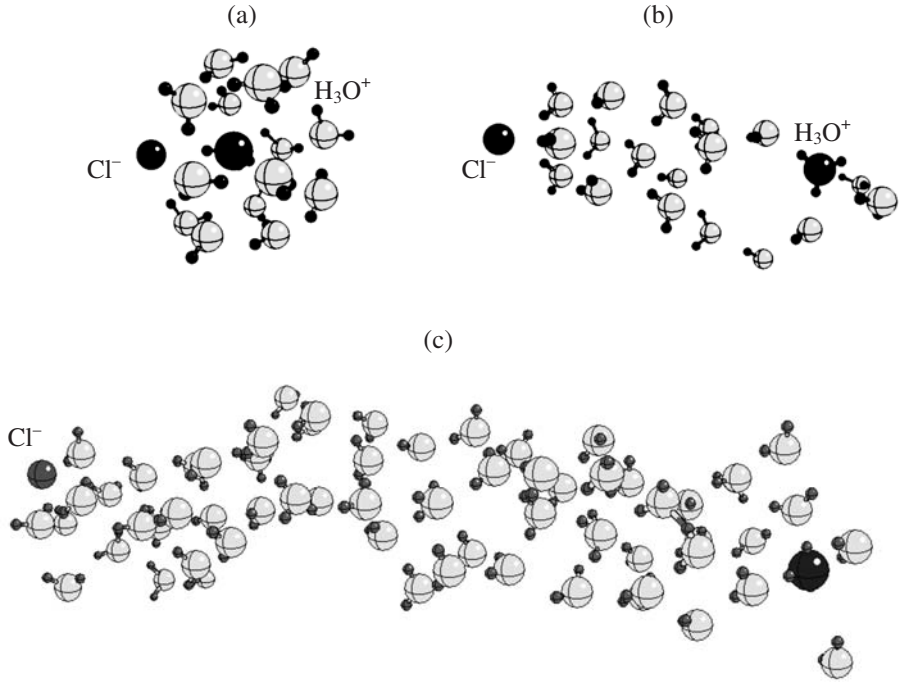

Fig. 2. Examples of configurations of the cluster $H_3O(H_2O)_4Cl^-$, obtained against the background of thermal fluctuations, for various interionic distances: (a) 3.4 Å (p = 1 kPa), (b) 14.1 Å (p = 300 Pa), and (c) 35.3 Å (p = 1 kPa).

$$Z_{rot}^{kin} = [(2k_BT)^{3/2}(I_1I_2I_3)^{1/2}\pi^{3/2}]/h^3. \quad (6)$$

Expression (5) is the result of integration over linear momenta in the statistical sum, and expression (6) is the result of integration over angular momenta of molecules; h, Planck constant; v_{ref}, arbitrary constant having the dimension of volume and setting the base for the configuration term of the chemical potential; σ, parameter of the rotational symmetry of a molecule (equal to 2 for water); and I_1, I_2, and I_3, its principal moments of inertia. To calculate each curve $\Phi(R)$, we generated a Markovian process consisting of 1.22×10^9 steps, of which 1×10^8 steps were attempts to shift water molecules with their turn (50–60% were accepted), 2×10^7 steps were attempts to shift hydroxonium ion with its turn (40–50% were accepted), and 10^9 steps were attempts to change the number of water molecules in the system (0.1–0.5% were accepted). Thus, the volume of the statistics for calculating $\Phi(R)$ was about 10^8 molecular configurations.The calculations were performed within a cavity of a radius of 50 Å, and then, for more detailed examination of the curve shape at short interionic distances, they were repeated within a cavity of a radius of 25 Å. The reproducibility of the calculated mean values was checked by duplicating calculations from various initial configurations.

Results of simulation of $H_3O^+(H_2O)_nCl^-$ in water vapor. Two qualitatively different relatively stable states of the hydration component of the complex $H_3O^+(H_2O)_nCl^-$ are observed. In the first state, the water molecules form a hydration shell around the $H_3O^+Cl^-$ ion pair (Fig. 2a), and in the second case the water molecules are drawn into the interionic space (Fig. 2b). The first, "enveloping" state corresponds to the global minimum, and the second, "internal" state, to the local minimum of the free energy. The enveloping states are realized at short interionic distances close to the contact distance, and the internal states, at interionic distances at which more than one water molecule can be accommodated between the ions. Fluctuation extensions of the interionic space are accompanied by drawing of vapor molecules into it; as a result, the hydration component acquires a strongly elongated shape (Fig. 3c) and remains stable (due to a network of hydrogen bonds) up to a certain maximal interionic distance depending on the vapor pressure, after which the chain is broken with the formation of two nonbonded cluster ions $H_3O^+(H_2O)_k$ and $Cl^-(H_2O)_m$,

with a significant part of the hydration component being evaporated ($k + m < n$). In the interionic space, .the hydration component of the cluster is strongly polarized, and its mean dipole moment differs from that in the case of full orientation ordering of dipole moments of the molecules by no more than 10%. The dipole moment of the hydration component of the cluster amounts to approximately 70% of the dipole moment of the ion pair and is oriented oppositely, so that the equilibrium mean dipole moment of the cluster has, on the average, the same direction as the dipole moment of the ion pair but is weakened by a factor of 3–4 by the hydration component.

The intermediate–strength potential $\Phi(R)$ has two minima separated by a high barrier (Fig. 3). Their positions depending on the vapor pressure are given in Table 1. The saturated vapor pressure over a planar phase boundary at 273 K is approximately 600 Pa. Therefore, the first four columns of the table correspond to unsaturated vapor, and the last column, to moderately supersaturated vapor. Similarly to the hydration shells of the H_3O+ [8, 10, 12, 14, 17] and Cl^- [2, 4, 6] ions, the hydration shell of the ion pair H_3O+Cl^- remains stable in moderately supersaturated water vapor. The first minimum at a distance $R^2_{\min(\Phi)}$ corresponds to contact interionic distance, i.e., to the recombined ion pair. Its position is almost independent of the vapor pressure. A slight shift of this minimum from 3.20 Å in unsaturated vapor to 3.25 Å in supersaturated vapor is associated with the addition of water molecules and was interpreted in [28] as an evidence of possible ionization of HCl molecules. However, actually only the second minimum at the interionic distance $R^2_{\min(\Phi)}$ corresponds to the dissociation of the molecules into the ions. The second minimum is more shallow and broader, and it is separated from the first minimum by a high barrier. The thermal energy k_BT at 273 K is 3.77×10^{-21} J. In the first row of Table 2 are the differences between the depths of these minima $\Delta\Phi_{2,1} = [\Phi(R^2_{\min(\Phi)}) - \Phi(R^1_{\min(\Phi)})]/k_BT$, expressed in k_BT units. Table 2 shows that the difference between the free energies $\Delta(R)$ in unsaturated vapor is enormous on the scale of thermal fluctuations, exceeding 100 k_BT. With an increase in the vapor density and in the cluster size, this difference decreases in supersaturated vapor to 56 k_BT, but this value is still too large for the fluctuating charge separation in the cluster under the conditions of thermodynamic equilibrium to become possible. The free energy $\Phi(R)$ is related to the conditions of a fixed

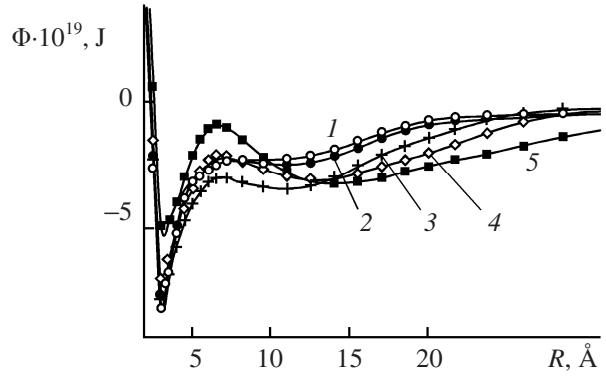

Fig. 3. Intermediate–strength interaction potential (accurate to constant summand) of H_3O+ and Cl^- ions as a function of the interionic distance in a cluster of water molecules occurring at 273 K in an equilibrium with water vapor at various pressures: (*1*) 3 Pa, (*2*) 10 Pa, (*3*) 30 Pa, (*4*) 300 Pa, and (*5*) 1 kPa.

Table 1. Positions,determined by spline interpolation, of the extrema of intermediate–strength ion interaction potential [$R_{\min}(\Phi)$, $R_{\max}(\Phi)$], internal energy of the cluster [$R_{\min}(U)$, $R_{\max}(U)$], entropy [$R_{\min}(S)$, $R_{\max}(S)$], equilibrium number of molecules in the cluster [$R_{\max}(n)$, $R_{\min}(n)$], and fluctuations of the number of molecules in the cluster [$R_{\max(\Delta n)}$, $R_{\min(\Delta n)}$] for the complex $H_3O+(H_2O)_nCl^-$ in water vapor at 273 K and various vapor pressures p

Parameter	Value, Å, at indicated p, Pa					
	3	10	30	100	300	1000
$R^1_{\min(\Phi)}$	3.20	3.21	3.21	3.22	3.23	3.25
$R_{\max(\Phi)}$	–	6.6	6.6	6.6	6.6	6.6
$R^2_{\min(\Phi)}$	–	10.6	11.5	12.4	13.3	14.2
$R^1_{\min(U)}$	4.4	4.3	4.2	4.1	4.0	3.8
$R_{\max(U)}$	6.5	6.4	6.4	6.3	6.3	6.2
$R^2_{\min(U)}$	14.0	16.1	18.2	20.3	22.5	28.6
$R^1_{\min(S)}$	3.0	2.9	2.8	2.7	2.6	2.4
$R_{\max(S)}$	6.4	6.3	6.3	6.2	6.2	6.1
$R^2_{\min(S)}$	14.5	15.4	17.6	20.2	21.8	27.8
$R^1_{\max(n)}$	4.6	4.3	4.1	3.9	3.7	3.5
$R_{\min(n)}$	6.4	6.3	6.3	6.2	6.2	6.1
$R^2_{\max(n)}$	15.1	16.3	17.8	19.3	22.2	28.3
$R^1_{\max(\Delta n)}$	4.1	3.8	3.6	3.4	3.2	3.1
$R_{\min(\Delta n)}$	6.1	5.9	5.9	5.8	5.7	5.4
$R^2_{\max(\Delta n)}$	18.5	20.8	23.3	26.1	28.9	33.5

Table 2. Difference between the depths of the free energy minima $\Delta\Phi_{2,1}$, height of the free energy barrier separating these minima $\Delta\Phi_b = [\Phi(R_{\max(\Phi)}) - \Phi(R^2_{\min(\Phi)})]/k_BT$, expressed in k_BT units, its half-width $\Delta R_{\max}(\Phi)$ in Å, ratio of the configuration volumes in the coordinate space of ions, corresponding to the separated and recombined charges, $\Omega_{2,1} = [(R^2_{\min(\Phi)})^2\delta R^2_{\min(\Phi}$ $[(R^1_{\min(\Phi)})^2\delta R^1_{\min(\Phi)}]$, probability of the fluctuation charge separation $w_{2,1}$, difference between the depths of the internal energy minima $\Delta U_{2,1} = [U(R^2_{\min(U)}) - U(R^1_{\min(U)})]/k_BT$, height of the internal energy barrier separating these minima $\Delta U_b = [U(R_{\max(U)})-$ $U(R^2_{\min(U)})]/k_BT$, expressed in k_BT units, and difference between the entropy minima $\Delta S_{2,1} = [S(R^2_{\min(S)}) - S(R^1_{\min(S)})]/k_BT$, expressed in k_B units, for the same system as in Table 1

Parameter	Value at indicated p, Pa					
	3	10	30	100	300	1000
$\Delta\Phi_{2,1}$	–	134	113	110	107	56
$\Omega_{2,1}$	–	148	154	193	237	324
$w_{2,1}$	–	9.4×10^{-57}	1.3×10^{-47}	3.3×10^{-46}	8.0×10^{-45}	1.5×10^{-22}
$\Delta\Phi_b$	–	4	13	19	27	62
$\delta\Phi_b$	–	3.4	3.8	5.2	5.8	6.1
$\Delta U_{2,1}$	–120	–138	–142	–190	–278	–595
ΔU_b	210	278	296	365	515	840
$\Delta S_{2,1}$	–229	–296	–344	–416	–568	–910

interatomic distance. The ratio of the configuration volumes associated with the relative mo-tion of ions is $\Omega_{2,1} = = [(R^2_{\min(\Phi)})^2\delta R^2_{\min(\Phi)}]/[(R^1_{\min(\Phi)})^2\delta R^1_{\min(\Phi)}]$, where $\delta R_{\min(\Phi)}$ is the half–width of the minimum corresponding to the locally stable state. The probability of the dissociation of a molecule into ions is estimated by Eq. (7):

$$w_{2,1} = \Omega_{2,1}\exp(-\Delta\Phi_{2,1}) . \quad (7)$$

As seen from the values of $w_{2,1}$ given in Table 2, the probability of dissociation into ions as a result of thermal fluctuations is negligible: The equilibrium amount of clusters with dissociated HCl molecules is by tens orders of magnitude smaller than that of the clusters containing nondissociated HCl molecules. The effect associated with the ion motion ($\Omega_{2,1}$) increases the probability of dissociation by only two orders of magnitude and cannot radically change the whole pattern. Although with an increase in the vapor pressure by two orders of magnitude (from 10 to 1000 Pa) the amount of dissociated molecules increases by 34 orders of magnitude, their relative amount is negligible even in supersaturated vapor (~10–22).

Thus, in the thermodynamically equilibrium state almost all the HCl molecules in water vapor occur in the nondissociated state. However, the amount of $H_3O{+}Cl^-$ ion pairs can sharply increase if there are external ionization sources. According to quantum–chemical calculations [28], the HCl covalent bond is cleaved at $n \geq 4$, but the ions are retained by electrostatic forces at a distance close to the contact distance, with the energy of the order $E_{sepr} \approx 8\times10^{-19}$ J. To break this bond, a quantum with the wavelength $\lambda = hc/E_{sepr}$ 2000 Å is required. This wavelength corresponds to the UV part of the solar radiation spectrum. Thus, hydration of molecules favors the cleavage of the covalent bond and shifts the ionization threshold toward longer wavelengths. The reverse recombination process starts with relatively slow cross diffusion of the couterions, and therewith the ions are hydrated and a molecular cluster is formed. In this cluster, the recombination decelerates because of a high barrier separating the ionized and nonionized states. The height of the free energy barrier $\Delta\Phi_b$ separating the absolutely stable state of the undecomposed molecule ($R^1_{\min(\Phi)}$) from the locally stable state of the HCl molecule that dissociated into ions ($R^2_{\min(\Phi)}$) ranges from several k_BT in strongly unsaturated vapor to tens of k_BT in supersaturated vapor, with the barrier half-width varying from 3 to 6 Å (Table 2).

In [39] a kinetic equation for cross dif-fusion of ions and estimated was obtained for the steady state of charge "pumping" from external ionizing radiation sources the amount of ion pairs stabilized in clusters of water molecules. The stationary solution of the equation and numerical estimations in [39] for $\Delta\Phi_b = 79.7$ (which corresponds to saturated vapor) lead to expression (8) for the ratio of the ion paris and unlinked hydrated ions and to expression (9) for the ratio of the ion pairs and undissociated HCl molecules:

$$\rho_2^s/\rho_1^s = 4.1\times10^{-25}\ (m^3)\cdot\exp(\Delta\Phi_b)\cdot\rho_1^s\ (m^{-3})$$

$$= 1.7\times10^{10}\ (m^3)\cdot\rho_1^s\ (m^{-3}) \quad (8)$$

$$\rho_2^s/\rho_{HCl}^s = 6.8\times10^{-32}\cdot\exp(\Delta\Phi_b) = 2.8\times10^3 \quad (9)$$

With an increase in the temperature from 200 to 273 K, the barrier width does not change noticeably, but its height $\Delta\Phi_b$ at saturated vapor pressure decreases, and the dependence on the vapor pressure becomes more pronounced with increasing temperature. At 273 K, in saturated vapor, $\Delta\Phi_b \sim 40$ (Table 2). Substitution of this value in Eqs. (8) and (9) gives expressions (10) and (11):

$$\rho_2^s/\rho_1^s = 9.8\times10^{-8}\ (m^3)\cdot\rho_1^s\ (m^{-3}) \quad (10)$$

$$\rho_2^s/\rho_{HCl}^s = 1.6\times10^{-14} \quad (11)$$

Comparison of Eqs. (8) and (9) with (10) and (11) shows that at stratospheric temperatures in saturated water vapor under the action of natural sources of ionizing radiation the following relationships between the contents of nonbonded hydrated charges (ρ_1^s), ion pairs (ρ_2^s), and nondissociated HCl molecules (ρ_{HCl}^s) are realized: $\rho_{HCl}^s << \rho_2^s >> \rho_1^s$, whereas at the temperature corresponding to normal conditions $\rho_{HCl}^s >> \rho_2^s << \rho_1^s$. At 273 K HCl molecules in clusters of water molecules occur in the nondissociated state, but after cooling to 200 K the ion pairs are accumulated. The dissociated state of HCl under stratospheric conditions is supported by two factors: generation of ions by ionizing radiation and inhibition of recombination in clusters by a high free energy barrier. The estimates made in [39] show that the time constant of ion pair accumulation can be enormous on the molecular scale and can reach months. At 273 K in unsaturated vapor, the barrier height is insufficient for the accumulation of ion pairs, but in a supersaturated vapor with a pressure of 1200 Pa, which corresponds to approximately twofold supersaturation, the barrier height in k_BT units reaches the same value as at 200 K in unsaturated vapor. Under these conditions, estimates (8) and (9) are valid, suggesting accumulation of clusters with nondissociated HCl molecules. In this case, the complexes $H_3O^+(H_2O)_nCl^-$ are in the metastable state whose lifetime depends on the state of the supersaturated vapor as a whole. Condensation of the supersaturated vapor will lead to a sharp decrease in its pressure, vaporization of a part of the hydration component of the complexes $H_3O^+(H_2O)_nCl^-$, and recombination of the counterions with the formation of an HCl molecule.

Thus, at 273 K the ion pairs $H_3O^+Cl^-$ can accumulate in clusters of water molecules only under the conditions of strongly supersaturated vapor, whereas at 200 K the ion pairs can accumulat in unsaturated water vapor also. With a decrease in the temperature from 273 to 200 K, the conditions concerning the degree of supersaturation become milder, and the lifetime of the metastable state of the vapor in which the accumulation of the ion pairs is possible rapidly increases. The boundary temperature at which the separated charges in the complexes $H_3O^+(H_2O)_nCl^-$ become retained for a macroscopic time is in the range from 273 to 200 K. Refinement of this value re-quires a considerable volume of additional compu-tations, but interpolation of the already obtained data gives grounds to expect a strong temperature dependence of the stability of the ion pairs in the temperature range ~210–250 K. Apparently, just the strong temperature dependence of the rate of accumulation of the ion pairs $H_3O^+Cl^-$, accelerating the adsorption of chloride ions on the surface of ice microcrystals in the stratosphere [40–45] is the cause of the observed seasonal cyclic recurrence of ozone decomposition in upper layers of the atmosphere [46–48]. The above-indicated interval falls within the range of temperature variation depending on the height over the Earth's surface. Because of the exponentially sharp dependence on the barrier parameters and temperature, the state of HCl can be essentially different depending on the season and height, which will affect the chain of fundamental physicochemical transformations.

Analysis of the energy and entropy terms gives insight into the mechanism of formation of extrema of the function $\Phi(R)$. The internal energy of a cluster $U(R)$ was calculated by direct averaging, separately for each discrete value of R_i. As in the calculation of $\Phi(R)$, we

constructed a nonuniform grid with smaller steps $R_i - R_{i-1}$ for small R.

The entropy of the cluster was calculated from the difference of $U(R)$ and $\Phi(R)$. Under the examined conditions, the vapor with a relatively high accuracy can be considered as an ideal gas. Since the simulation conditions correspond to a constant vapor pressure (NpT statistical ensemble [38]), the intermediate-strength potential $\Phi(R)$ coincides, to a constant summand, with the Gibbs energy of the system as a whole. The potential $\Phi(R)$ is related to the internal energy by expression (12) neglecting the volume occupied by the cluster compared to the volume per molecule in the gas phase:

$$\begin{aligned}\Phi(R) &= U(R) - TS_{\mathrm{cl}}(R) - T[N - \langle n(R)\rangle]s_{\mathrm{g}} \\ &\quad + p[N - \langle n(R)\rangle]v_{\mathrm{g}} + \mathrm{const} \\ &= U(R) - TS(R) - \langle n(R)\rangle k_{\mathrm{B}}T + \mathrm{const}, \qquad (12)\end{aligned}$$

where N is the total number of molecules in the cluster and in water vapor; $<n(R)>$, mean number of molecules in the cluster; $S_{\mathrm{cl}}(R)$, cluster entropy; $U(R)$, con-figuration term of the internal energy of the cluster; s_{g}, entropy; and v_{g}, volume per molecule in the gas phase. The entropy of the cluster, counted from the entropy of the corresponding number of molecules in the gas phase, $S(R) = S_{\mathrm{cl}}(R) - <n(R)>s_{\mathrm{g}}$, is obtained from (12) in form (13):

$$S(R) = [U(R) - \Phi(R)]/T - \langle n(R)\rangle k_{\mathrm{B}} + \mathrm{const}. \qquad (13)$$

The quantity S(R) is the configuration term of the entropy, because the contributions to $S_{\mathrm{cl}}(R)$ and $<n(R)>s_{\mathrm{g}}$ associated with the integration over the momenta subspace coincide, and the corresponding contributions to S(R) decrease.

As in the case of $\Phi(R)$ there are two minima in the $S(R)$ curve separated by a maximum, but the positions of the extrema of S(R) and $\Phi(R)$ do not coincide (Table 1): The first minimum of S(R) cor-responds to somewhat shorter distances, and with increasing pressure the first minimum of $\Phi(R)$ shifts toward larger values and the minimum of S(R), on the contrary, toward smaller values; the difference $R^1_{\min(\Phi)} - R^1_{\min(S)}$ at a pressure of 1000 Pa reaches 30%. The se-cond minima of S(R) and $\Phi(R)$ both shift toward larger values with increasing pressure, but that of S(R) shifts approximately two times faster (Table 1). The maxi-mum of S(R) slightly shifts toward smaller values with increasing pressure, and the maximum of $\Phi(R)$ remains on the same position. The dependences of the positions of the extrema of $U(R)$ and $<n(R)>$ on the vapor pressure are qualitatively the same as for S(R), with a slight shift toward larger values (Table 1).

The extrema in the dependence $U(R)$ are considerably more pronounced than in $\Phi(R)$ (Table 2). For example, the barrier height (in $k_{\mathrm{B}}T$ units) varies in the examined range of conditions from 240 to 840 for $U(R)$ and from 4 to 62 for $\Phi(R)$. The barrier in $\Phi(R)$ decreases, according to (12), mainly owing to the entropy term; the contribution of the term $<n(R)>k_{\mathrm{B}}T$ is not decisive here and varies from $5k_{\mathrm{B}}T$ to 50 $k_{\mathrm{B}}T$ respectively. In the dependence $U(R)$ the second minimum is considerably deeper than the first minimum, whereas in $\Phi(R)$, on the contrary, the first minimum is deeper. Replacement of $\Phi(R)$ by $U(R)$ even in approximate estimates would lead to a essentially erroneous conclusion that the dissociated state of HCl is absolutely stable; here the entropy term plays a key role. An inversion of the relationship between the depths of the minima of $\Phi(R)$, compared to $U(R)$, is due to the larger depth of the second minimum of $S(R)$ (Fig. 4), with the difference between the second and first minima in the dependence $TS(R)$ being more pronounced than in $U(R)$. It is the very low entropy in the region of the second minimum that deprives of the absolute stability the dissociated states of the HCl molecule.

The fluctuations of the cluster size are strongly correlated with the fluctuations of the interionic distance. In Fig. 5 the mean number of water molecules in the cluster is plotted vs interionic distance. In the $<n(R)>$ curve there are two maxima corresponding to the minima in the dependences U(R), S(R), and $\Phi(R)$. The extrema of $<n(R)>$ coincide most closely in the position with the extrema of $U(R)$ (Table 1). The first maximum in $<n(R)>$ corresponds to the enveloping state of the hydration component of the cluster, and the second maximum, to the hydration component drawn into the interionic space. The minimum corresponds to the transition state between these two essentially different states. The largest size of the hydration shell is attained at the interionic distance exceeding by 1.5 Å the contact distance (Table 1). This effect is due to an increase in the dipole moment and to enhancement of the electric field as the ions are drawn apart. A shift of this minimum toward shorter distances with increasing pressure (Fig. 5b) is due to increased probability of drawing of molecules

into the interionic space in a denser vapor and to stimulation of the rearrangement into the state with the molecules drawn into the interionic space. An increase in the interionic distance to values larger than $R^2_{\max(n)}$ is accompanied by the loss of a part of molecules (Fig. 5a), by break of the hydration bridge, and by formation of two non-bonded hydrated ions. Increasing fluctuations of the number of molecules in the cluster $\Delta n(R) = [<n^2(R)> - <n(R)^2>]^{1/2}$ (Fig. 6) suggest the instability of the hydration component with respect to both uptake and loss of water molecules. The first maximum of $<n(R)>$ is located to the left of the first maximum of $<n(R)>$, in the region of rapid growth of the number of molecules in the cluster as the ions are drawn apart from the contact distance (Table 1). The second maximum of $\Delta n(R)$ is located to the right of the second maximum of $<n(R)>$. Increasing fluctuations in this region accompany the break of the cluster as a whole into two nonbonded hydrated ions. The interval of the interionic distances from 6 to 20 Å correspond to the region of the highest stability of the hydration component. Variations of the position of the second minimum of the intermediate–strength po-tential (Table 1), responsible for the stable position of the

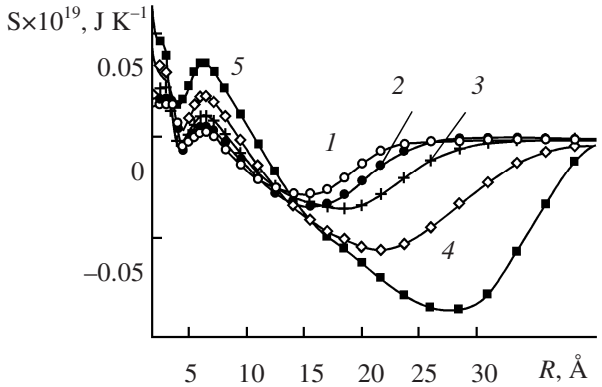

Fig. 4. Entropy (accurate to a constant summand) of the combined system of the cluster $H_3O+(H_2O)_nCl^-$ and vapor occurring in equilibrium with it, under the same conditions as in Fig. 3.

ions, are restricted by the same limits. Thus, the ions and hydration component in an equilibrium with the vapor attain the stable state simultaneously, but the states with the maximal number of molecules captured from the vapor are not the most stable.

The HCl molecules in water vapor are hydrated to form an enveloping shell, or the water molecules are drawn into an interionic space. The two types of states

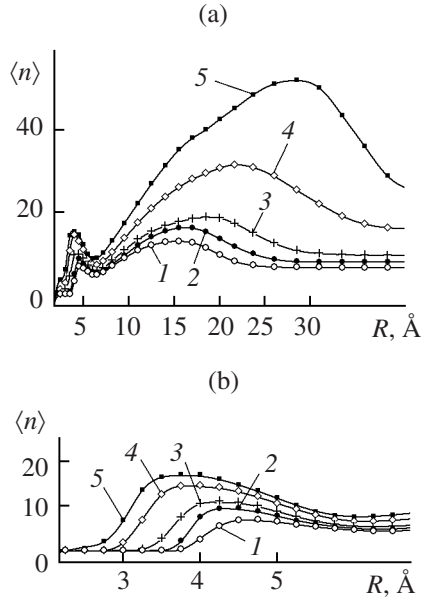

Fig. 5. Equilibrium number of water molecules in the cluster $H_3O+(H_2O)_nCl^-$ under the same conditions as in Fig. 3: (a) in a wide range of interionic distances and (b) at short interionic distances.

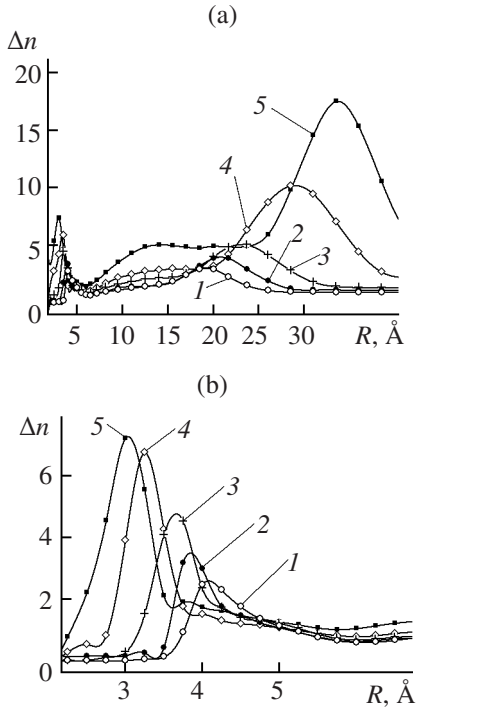

Fig. 6. Fluctuations of the number of water molecules in the cluster$H_3O+(H_2O)_nCl^-$ under the same conditions as in Fig. 3: (a) in a wide range of interionic distances and (b) at short interionic distances.

are separated by an energy barrier, and transition from one type to another is accompanied by the loss of a part of the hydration component. The clusters containing HCl are stable in a wide range of conditions. The dissociated form of HCl has a lower energy in clusters than the molecular form, but the molecular form is absolutely stable in clusters of water molecules irrespective of the vapor pressure. This fact is due to the low entropy of the system containing clusters with HCl in the ionized form. Nevertheless, the state of dissociation into ions is relatively stable. It corresponds to a local minimum of the free energy (Gibbs energy), separated from the state of the molecular form by a high barrier. The barrier height strongly depends on the temperature and vapor pressure in equilibrium with the cluster. At 200 K, the barrier parameters are sufficient for the inhibition of the recombination and for the accumulation of ion pairs that were generated by ionization under the action of natural sources of ionizing radiation and have not recombined in the clusters. At 273 K, the barrier height is insufficient to appreciably inhibit the recombination, and the ion pairs are not accumulated. In water vapor in the temperature range 210–250 K, under the conditions of natural ionizing radiation, the state of HCl changes qualitatively from the ionized form to the molecular form.

Along with the ionizing radiation, a possible source of nonrecombined ion pairs $H_3O^+Cl^-$ that are accumulated in clusters is evaporation from a liquid surface film of ice where dissolved HCl occurs in the dissociated form. The contribution of this mechanism depends on the ratio of the rates of recombination and cluster formation in the transition layer at the ice surface, and this matter requires a detailed kinetic study [49].

ACKNOWLEDGMENTS

The study was supported by the Russian Foundation for Basic Research (project no. 07–03–00103–a).

REFERENCES

1. Shevkunov, S.V., *Elektrokhimiya*, 1996, vol. 32, no. 8, p. 942.
2. Shevkunov, S.V., *Kolloidn. Zh*., 2002, vol. 64, no. 2, p. 262.
3. Shevkunov, S.V., *Zh. Fiz. Khim*., 2002, vol. 76, no. 4, p. 583.
4. Shevkunov, S.V., *Khim. Fiz*., 2003, vol. 22, no. 1, p. 90.
5. Shevkunov, S.V., Lukyanov, S.I., and Milot, Cl., *Chem. Phys.,* 2005, vol. 310, nos. 1–3, p. 97.
6. Lukyanov, S.I., Zidi, Z.S., and Shevkunov, S.V., *J. Mol. Struct. (THEOCHEM)*, 2005, vol. 725, nos. 1–3, p. 191.
7. Shevkunov, S.V., *Zh. Eksp. Teor. Fiz*., 1994, vol. 105, no. 5, p. 1258.
8. Shevkunov, S.V., *Dokl. Ross. Akad. Nauk,* 1998, vol. 363, no. 2, p. 215.
9. Shevkunov, S.V., *Elektrokhimiya*, 1998, vol. 34, no. 8, pp. 860, 869.
10. Shevkunov, S.V., *Khim. Vys. Energ*., 1999, vol. 33, no. 5, p. 325.
11. Shevkunov, S.V. and Vegiri, A., *J. Chem. Phys.,* 1999, vol. 111, no. 20, p. 9303.
12. Shevkunov, S.V. and Vegiri, A., *Mol. Phys*., 2000, vol. 98, no. 3, p. 149.
13. Vegiri, A. and Shevkunov, S.V., *J. Chem. Phys.,* 2000, vol. 113, no. 19, p. 8521.
14. Shevkunov, S.V., *Kolloidn. Zh*., 2000, vol. 62, no. 4, p. 569.
15. Shevkunov, S.V., *Zh. Obshch. Khim.*, 2002, vol. 72, no. 5, p. 735.
16. Shevkunov, S.V., *Zh. Obshch. Khim*., 2004, vol. 74, no. 9, p. 1409.
17. Shevkunov, S.V., *Zh. Obshch. Khim*., 2004, vol. 74, no. 10, p. 1585.
18. Shevkunov, S.V., *Zh. Obshch. Khim.*, 2004, vol. 78, no. 10, p. 1808.
19. Carlon, H.R., *J. Appl. Phys*., 1981, vol. 52, no. 5, p. 3111.
20. Carlon, H.R., *Appl. Opt*., 1981, vol. 20, no. 8, p. 1316.
21. Carlon, H.R., *J. Appl. Phys*., 1981, vol. 52, no. 4, p. 2638.
22. Carlon, H.R., *J. Chem. Phys*., 1982, vol. 76, no. 11, p. 5523.
23. Carlon, H.R., *J. Chem. Phys.*, 1983, vol. 78, no. 3, p. 1622.
24. Shevkunov, S.V., *Kolloidn. Zh*., 2004, vol. 66, no. 2, p. 248.
25. Lau, Y.K., Ikuta, S., and Kebarle, P., *J. Am. Chem. Soc*., 1982, vol. 104, no. 6, p. 1462.
26. Arshadi, M., Yamdagni, R., and Kebarle, R., *J. Phys. Chem*., 1970, vol. 74, no. 7, p. 1475.
27. Hiroaka, K., Mizuse, S., and Yamade, S., *J. Phys. Chem*., 1988, vol. 92, no. 13, p. 3943.
28. Re, S., Osamura, Yo., and Suzuki, Y., *J. Chem. Phys.*, 1998, vol. 109, no. 3, p. 973.
29. Feynman, R.P. and Hibbs, A.R., *Quantum Mechanics and Path Integrals*, New York: McGraw–Hill, 1965.

30. Shevkunov, S.V. and Vorontsov–Velyaminov, P.N., *Mol. Simulat*., 1991, vol. 7, p. 249.
31. Shevkunov, S.V., *Dokl. Ross. Akad. Nauk*, 1999, vol. 369, no. 1, p. 43.
32. Shevkunov, S.V., *Dokl. Ross. Akad. Nauk*, 2002, vol. 382, no. 5, p. 615.
33. Shevkunov, S.V., *Zh. Eksp. Teor. Fiz*., 2005, vol. 127, no. 3, p. 696.
34. Shevkunov, S.V., *Zh. Eksp. Teor. Fiz*., 2006, vol. 130, no. 1 (7), p. 105.
35. Shevkunov, S.V., *Dokl. Ross. Akad. Nauk*, 2006, vol. 409, no. 2, p. 176.
36. Shevkunov, S.V., *Zh. Vychisl. Matem. Matem. Fiz*., 2005, vol. 45, no. 12, p. 2283.
37. Shevkunov, S.V., *Kolloidn. Zh.*, 2004, vol. 66, no. 4, p. 554.
38. Hill, T.L., *Statistical Mechanics. Principles and Selected Applications*, New York: McGraw–Hill, 1956.
39. Shevkunov, S.V., *Kolloidn. Zh*., 2004, vol. 66, no. 4, p. 566.
40. Thibert, E. and Domine, F., *J. Phys. Chem. B*, 1997, vol. 101, no. 18, p. 3554.
41. Donsig, H.A., Herridge, D., and Vickerman, J.C., *J. Phys. Chem. A*, 1998, vol. 102, no. 13, p. 2302.
42. Doeppenschmidt, A., Kappl, M., and Butt, H.J., *J. Phys. Chem. B*, 1998, vol. 102, no. 40, p. 7813.
43. Isakson, M.J. and Sitz, G.O., *J. Phys. Chem. A*, 1999, vol. 103, no. 13, p. 2044.
44. Bluhm, H. and Salmeron, M., *J. Chem. Phys*., 1999, vol. 111, no. 15, p. 6947.
45. Fluckiger, B., Chaix, L., and Rossi, M.J., *J. Phys. Chem.*, 2000, vol. 104, no. 50, p. 11739.
46. Solomon, S., Garcia, R.R., Rowland, F.S., and Wuebbles, D.J., *Nature*, 1986, vol. 321, no. 6072, p. 755.
47. Molina, M.J., Tso, T.–L., Molina, L.T., and Wang, F.C.Y., *Science*, 1987, vol. 238, no. 4831, p. 1253.
48. Clary, D.C., *Science*, 1996, vol. 271, no. 5255, p. 1509.
49. Fisenko, S.P., Kane, D.B., and El–Shallc, M.S., *J. Chem. Phys*., 2005, vol. 123, no. 10, p. 104704.